N 62 62514

RM E54A08

NACA RM E54A08

NACA

RESEARCH MEMORANDUM

EXPERIMENTAL INVESTIGATION OF ROTATING STALL AND BLADE VIBRATION IN THE AXIAL-FLOW COMPRESSOR OF A TURBOJET ENGINE

By Merle C. Huppert, Howard F. Calvert, and André J. Meyer

Lewis Flight Propulsion Laboratory
Cleveland, Ohio

NATIONAL ADVISORY COMMITTEE FOR AERONAUTICS

WASHINGTON

April 26, 1954
Declassified April 15, 1958

NATIONAL ADVISORY COMMITTEE FOR AERONAUTICS

RESEARCH MEMORANDUM

EXPERIMENTAL INVESTIGATION OF ROTATING STALL AND BLADE VIBRATION IN THE AXIAL-FLOW COMPRESSOR OF A TURBOJET ENGINE

By Merle C. Huppert, Howard F. Calvert, and André J. Meyer

SUMMARY

A compressor-blade-vibration survey was conducted on a production turbojet engine incorporating an axial-flow compressor with a pressure ratio of approximately 7. Resistance wire strain gages were used to measure the vibratory stress in the first-stage rotor blades, and the flow fluctuations due to rotating stall were detected and measured by use of the constant-temperature hot-wire anemometer. The investigation was conducted with three different guide-vane assemblies and four jet-nozzle sizes. High vibratory stresses were measured in two distinct speed ranges. The cause of the high vibratory stresses in both speed ranges was determined to be resonant excitation due to rotating stall.

INTRODUCTION

Fatigue failures of compressor blades due to vibration has been a major problem in the development of axial-flow compressors. In general, the vibration of compressor blades have been considered to be one of two types: (1) forced vibration, or (2) self-excited vibration (flutter).

Forced vibrations of rotor blades due to wakes from struts or other objects in the air stream are generally prevented or eliminated by careful design. It has recently been established that stall of compressor-blade rows may result in the formation of low-flow zones in the compressor annulus (see refs. 1 to 5). These low-flow zones generally propagate at a uniform rate from blade to blade in the direction of rotor rotation, and, consequently, the phenomenon has been named rotating stall. The data of references 4 and 5 show that rotating stall may be a source of forced vibration excitation in both rotor and stator blades.

Several forms of self-excited or flutter-type vibration are evidently possible (ref. 6). Of the various types of flutter, stall flutter seems to be of greatest interest. The correlation between flutter-cascade results and compressor blade vibrations is not, however, generally satisfactory (ref. 7).

The data of reference 5 and the discussion of reference 8 indicate that the flow fluctuations of rotating stall may exist in a multistage compressor over an appreciable portion of its operating range up to 70 or 80 percent of design speed. Inasmuch as the stall zones may extend throughout the axial length of the compressor, the fluctuations of rotating stall may be a source of vibration excitation in all stages. Presumably, if the excitation frequency of the rotating stall were to be equal to or some fraction of the natural frequency of any of the blades, a resonant vibration would occur. The amplitude of the resulting vibratory stress would, of course, depend on the strength of the excitating force due to rotating stall and the amount of damping in the blading. Information on the relation between rotating stall and vibration problems in current production turbojet engines is lacking at present.

The investigation reported herein was conducted to determine the rotating stall patterns obtainable in the compressor of a production turbojet engine, and to determine if the flow fluctuations of rotating stall could excite sufficiently high vibratory stresses in the blading to result in fatigue failure. The flow fluctuations of rotating stall were detected and measured by use of a constant-temperature hot-wire anemometer. The vibratory stresses in the first-rotor blades were measured by use of resistance wire strain gages.

APPARATUS AND PROCEDURE

Apparatus

Turbojet engine. - The investigation was conducted in a sea-level static test stand using a production turbojet engine incorporating an axial-flow compressor with a pressure ratio of approximately 7. The engine reportedly had some history of blade failures in the first-stage aluminum-alloy rotor blades. The failures had occurred in the engine-speed range between 50 and 70 percent of rated engine speed.

In order to vary the stall in the inlet stages, four different jet-nozzle areas and three different inlet-guide-vane assemblies were used. The largest jet-nozzle area used in this investigation was that which produced the rated turbine discharge temperature at the rated engine speed and is hereinafter referred to as the standard jet nozzle. The other three jet-nozzle sizes were 4, 8, and 12 percent smaller than the standard. The three guide-vane assemblies were made of identical blades. Only the solidity and blade setting angles were changed. Figure 1 presents the estimated variation in guide-vane turning angle with radius for the three guide-vane assemblies. The blading solidity is the same at all radii. The estimates of guide-vane turning were based on measurements of the blades. The flow deviation angles at the guide-vane discharge were computed using Constant's rule for deviation (ref. 9).

The various engine configurations investigated incorporated combinations of the three guide-vane assemblies and four jet-nozzle sizes. The seven configurations used are identified and listed in table I. Hereinafter, the engine configuration will be referred to by number.

Methods of detecting and measuring vibratory stress. - Commercial resistance wire strain gages were cemented to 12 first-stage compressor rotor blades at the midchord position as close as possible to the blade base and lead wires were run across the face of the first-stage disks to the center line of the compressor, and then through the shaft to a 19-ring slip-ring assembly. The instrumented blades were in three approximately equally spaced groups of four blades each. The slip-ring assembly and strain-gage circuits were the same as reported in reference 10.

In addition, a permanent magnet was mounted in the tip of one blade each in the first-, second-, and third-stage rotors. Circumferential slots were machined on the inside of the compressor case with their center lines over the center line of each of the first three rotors. A wire coil was installed in each slot with the wires placed circumferentially in the casing of the compressor as shown in figure 2. Inasmuch as the rotor blades are set at an angle with respect to the compressor axis of rotation, any blade vibration would cause the magnetic field due to the magnets in the blades to cut the coils, resulting in an electromotive force generated in the coil. The voltage output is proportional to the rate of cutting flux or to the blade velocity normal to the coil wires, and is consequently a measure of the amplitude of the blade motion in and out of the plane of rotation due to vibration. This device will hereinafter be referred to as a magnetic vibration indicator.

A 12-channel recording oscillograph was used to record the strain-gage and magnetic-vibration indicator signals along with hot-wire-anemometer signals. The hot-wire-anemometer system used will be discussed in the following section.

The fundamental bending frequencies of the rotor blades in the first three stages were determined experimentally and are listed in the following table. The values for the magneted blades used with the magnetic-vibration indicator are also listed:

Stage	Average frequency of standard blades, cps	Frequency of blades with magnet, cps
1	178	163
2	226	205
3	286	251

Hot-wire anemometer. - The constant-temperature hot-wire-anemometer system discussed in reference 11 was used to detect rotating stall. The anemometer probes were wired with 0.0002-inch-diameter tungsten wire with an effective length of 0.08 inch. For most of the data obtained, the wire element was perpendicular to the radial direction and oriented normal to the mean flow direction, and in some cases, probes with radial wire elements were used. Anemometer probes were installed in radial survey devices located in the first-, second-, and third-stage stator passages. Three angular spacings of the anemometer probes (approx. 30°, 60°, and 90°) were provided.

The anemometer signals were filtered to eliminate frequencies greater than 750 cycles per second and viewed two at a time on a dual-beam direct-coupled cathode-ray oscilloscope and recorded by photographing the oscilloscope and/or by use of the 12-channel recording oscillograph used for recording the vibration record.

The method used for determining the number of stall zones in the stall patterns and the amplitude of the flow fluctuation was that outlined in reference 3. The frequency f_s with which the stall zones passed an anemometer probe was determined by the technique of forming Lissajous figures with the aid of an audio frequency oscillator (see ref. 12, for example) and in some cases by use of the oscillograms obtained with the 12-channel recording oscillograph. Good agreement was obtained between the frequencies determined by the two methods.

Procedure

The investigation was conducted in a sea-level static test stand. The engine was first operated at rated speed with guide-vane assembly A (see fig. 1) to establish the jet-nozzle area that resulted in rated turbine discharge temperature at rated speed. This jet-nozzle area is referred to as the standard jet-nozzle size in table I. The engine was then operated with the standard jet nozzle and the standard inlet guide vanes (configuration 1, see table I) at each of several rotational speeds from approximately 40 to 100 percent of rated speed. The flow fluctuations of rotating stall were detected at all speeds below about 70 percent of design, but the vibratory stresses in the first rotor did not exceed 5000 pounds per square inch. An engine acceleration run, however, produced vibratory stresses of 13,000 pounds per square inch in the first-stage rotor at about 62 percent of design speed. In an attempt to obtain the conditions within the compressor during steady-stage operation that produced the blade vibrations during engine acceleration, data were then obtained with reduced jet-nozzle area, that is, configurations 2, 3, and 4 (table I).

To further vary the degree of stall in the inlet stages, reduced guide-vane turning was investigated along with various jet-nozzle sizes (configurations 5, 6, and 7, table I).

RESULTS AND DISCUSSION

The stall patterns detected and the vibratory stresses observed will first be discussed separately and then the correlation between the frequency of the flow fluctuations relative to the rotor due to rotating stall and the rotor-blade vibratory frequency will be discussed.

Stall Patterns

Rotating stall patterns were observed in all engine configurations investigated. The flow fluctuations due to stall were confined largely to the annular area between the rotor-blade pitch line and the rotor tip, and consequently could be classified as a progressive stall as discussed in reference 8.

The amplitude of the flow fluctuations varied considerably with time. Under some conditions, generally below 50 percent of design speed, the stall patterns were difficult to identify. Oscillograms obtained from the dual-beam oscilloscope showing typical hot-wire-anemometer signals are presented in figure 3, and the engine conditions are tabulated on the figure.

The stall frequencies f_s and the number of stall zones in the stall patterns observed with each engine configuration will be discussed in the following sections.

Configuration 1 (standard guide vanes and jet nozzle). - With engine configuration 1, the flow fluctuations due to rotating stall were the largest in the third-stage stators, and consequently, the hot-wire anemometers were placed at this location for determining the stall frequency and the number of zones in the stall patterns. Figure 4(a), which is a plot of the stall frequency against percent of design speed, summarizes the stall data obtained with this configuration. Between 48 to 71 percent of design speed, stall patterns with four zones were observed, and between 58 and 68 percent of design speed stall patterns with five zones were also detected. In the speed range between 58 and 68 percent of design speed, the number of zones was intermittently changing between four and five. The four-zone pattern was predominate except for the speed range between 61 and 65 percent design speed when the five-zone pattern appeared a major part of the time. Above approximately the 71 percent speed, rotating stall was not detected. For each stall pattern, the stall frequency is approximately proportional to engine speed.

Configurations 2, 3, and 4 (standard guide vanes, reduced jet-nozzle area). - The effect of operating the engine with configurations 2, 3, and 4 was to cause the four- and five-zone stall patterns to persist over a larger speed range up to 73 percent of design speed. It also appeared that the flow fluctuations increased in amplitude with reduced jet-nozzle area.

Configuration 5 (guide-vane assembly B, standard jet nozzle). - The reduced turning in the guide vane resulted in an increase in the radial extent of the stall in the first-stage stator and an appreciable decrease in the amplitude of the flow fluctuation in the third stage. The stall zones extended from the tip to the midspan position in the first-stage stators. Stall patterns with four, five, and six stall zones were detected. The stall patterns with four and five stall zones were detected over the same speed range as they occurred with configurations 1, 2, 3, and 4. The stall pattern with six stall zones was detected in the speed range between 60 and 65 percent of design speed. In this speed range, the number of zones in the stall pattern changed intermittently among four, five, and six. With this configuration, the compressor was free of stall patterns above about 67 percent of design speed.

Configuration 6 (guide-vane assembly B, jet-nozzle area reduced 8 percent from standard). - Figure 4(b) presents the stall data obtained with configuration 6. The number of zones in the stall patterns was the same as for configuration 5. However, the reduction in jet-nozzle area caused the stall pattern to persist up to 73 percent of design speed.

Configuration 7. - The stall patterns observed with configuration 7 were the same as those for configuration 6 (fig. 4(b)) except that the six-zone pattern was not readily detectable. Before complete anemometer data could be obtained, a fatigue failure was experienced in a first-stage rotor blade, terminating the investigation.

Stress Measurements

Steady-state operation with configuration 1 did not produce vibratory stresses in the standard first-stage rotor blades greater than ±5000 pounds per square inch under any condition. Inasmuch as the 5,000,000-cycle endurance limit for the material is about ±16,000 pounds per square inch, stresses of this magnitude are considered unimportant. An engine acceleration run, however, resulted in short bursts of vibrations with a maximum stress of ±13,500 pounds per square inch at approximately 62 percent of design speed. An oscillogram showing one of these short bursts of vibration in four standard first-stage rotor blades is given in figure 5. The first-stage rotor blade with the magnet installed at its tip was observed to vibrate with a stress of ±21,000 pounds per square inch at an engine speed (steady speed) of 67 percent of design speed. Inasmuch as the magnet installed in the rotor tip reduced the natural bending frequency of the blade, the vibrational characteristics were not expected to be the same as the standard blades. No vibration was observed in the other first-stage blades as the engine speed was increased above 67 percent of the design speed.

A plot of the vibratory stress against percent of design speed obtained with configuration 3 is shown in figure 6. It can be readily seen that two critical speeds are present over the speed range from 58 to 72 percent of design speed. Also note that the "magneted" blade reached its maximum vibratory stress at a lower speed than the standard blade.

After these two critical speeds were observed, the balance of the investigation was guided to determine their cause. Operation with configuration 4 resulted in vibratory stress of ±34,800 pounds per square inch in the high critical speed range (70 percent of design speed), and was the highest vibratory stress measured during the investigation.

Operation with reduced guide-vane turning (configurations 5, 6, and 7) also resulted in high vibratory stresses in the first-stage rotor blades at the two critical engine speeds. A summary of the stresses measured in the standard first-stage rotor blades is presented in table II. All vibrations observed were of the bursting or spasmodic type, and the number of cycles in the burst varied from 10 to approximately 350. In general, the greater the vibratory stress, the longer the vibration persisted. For example, the vibration burst illustrated in figure 6 and obtained with configuration 1 during an engine acceleration had a duration of about 13 stress cycles, and with configuration 5, the maximum vibratory stress (34,500 lb/sq in.) was measured during a burst of about 350 cycles. Figure 7 is a typical oscillogram of a long burst of high vibratory stress for five standard first-stage rotor blades. The operating condition under which the vibrations were encountered are noted on the figure.

CORRELATION OF ROTATING STALL AND BLADE VIBRATION

The frequency of excitation due to rotating stall for the rotor blade is the stall frequency relative to the rotor blade. The absolute stall frequency f_s as determined from the hot-wire-anemometer signals is related to the stall frequency relative to the rotor f_s' by the following formula:

$$f_s' = N\lambda - f_s$$

where

N engine speed, rps

λ number of stall zones in stall pattern

The stall frequency relative to the rotor f_s' for the seven engine configurations investigated is presented as a function of rated engine speed in figure 8. As can be seen from figure 8, the stall frequencies relative to the rotor for a given stall pattern obtained with configurations 1 through 4 are slightly greater than those obtained with configurations 5 through 7 at engine speeds above 50 percent of rated speed. As pointed out previously, a stall pattern with six zones was not found with configurations 1 through 4.

In order to establish whether the blade vibrations obtained were excited by rotating stall, the stall frequency relative to the rotor f_s' was compared with the blade vibration frequencies. The principal results of the comparison are shown in figure 9. The vibrational frequencies of the first-stage rotor blades and the stall frequency relative to the rotor are plotted against percent of rated speed. In addition, the calculated variation of the average natural frequency of the standard first-stage rotor blades with engine speed is shown. The variation of bending frequency among the first-stage rotor blades was about ± 5 cycles per second. The effect of engine speed on the natural bending frequency was estimated by the method presented in reference 13.

Good correlation between the five-zone stall frequency relative to the rotor and the blade vibrational frequency is indicated at engine speeds between about 65 and 72 percent of rated engine speed. This correlation indicates that the blades were excited by rotating stall. Examination of the oscillogram records indicated the time duration of the bursts of vibration corresponded to the time a five-stall pattern was present in the compressor. As mentioned earlier, the stall patterns were changing intermittently. The magnitude of the vibration stresses of each circled point in figure 9 is shown in figure 6.

Good correlation was also obtained for the vibrations excited with configuration 5 at 62 percent of design speed. The data show that the high vibratory stresses excited were caused by the stall pattern with six stall zones. As was the case with the five-zone stall pattern, the duration of the bursts of vibration corresponded to the existence of the six-zone stall pattern.

The blade vibrations excited in configurations 1 through 4 in the speed range between 58 and 63 percent of rated speed correlate well with the estimated relative stall frequency for a six-zone stall pattern. At a given engine speed, estimated relative stall frequency for six zones is taken to be six-fifths of the relative stall frequency for the five-zone stall pattern. A six-zone stall pattern, however, was not detected with these configurations. Inasmuch as the duration of the vibration

bursts was short, between 13 to 30 cycles, the time that the six-stall zone would be present is approximately 0.1 second. The Lissajous method used for determining frequency was not suitable for determining the frequency of a stall pattern for such a short duration. It seems reasonable, however, to assume that rotating stall was responsible for these low-amplitude vibrations as well as the high-amplitude vibrations.

SUMMARY OF RESULTS

A compressor-blade-vibration survey was conducted on a production turbojet engine incorporating an axial-flow compressor with a pressure ratio of approximately 7. Resistance wire strain gages were used to measure the vibratory stress in the first-stage rotor blades, and the flow fluctuations due to rotating stall were detected and measured by use of the constant-temperature hot-wire anemometer. The investigation was conducted using three different guide-vane assemblies and four jet-nozzle sizes. Vibratory stresses greater than ±20,000 pounds per square inch were encountered in two distinct ranges of engine speed. The low-speed range is at approximately 62 percent of rated engine speed and the high-speed range at approximately 70 percent of rated speed. The excitation of these high-amplitude vibrations was determined to be rotating stall. The vibratory stresses exceeded the endurance limit of the blading material, and the investigation was terminated by a fatigue failure of a first-stage rotor blade.

Lewis Flight Propulsion Laboratory
National Advisory Committee for Aeronautics
Cleveland, Ohio, January 7, 1954

REFERENCES

1. Iura, T., and Rannie, W. D.: Observations of Propagating Stall in Axial-Flow Compressors. Rep. No. 4, Mech. Eng. Lab., C.I.T., Apr. 1953. (Navy Contract N6-ORI-102, Task Order 4.)

2. Emmons, H. W., Pearson, C. E., and Grant, H. P.: Compressor Surge and Stall Propagation. Paper No. 53-A-65, presented at A.S.M.E. meeting, 1953.

3. Huppert, Merle C.: Preliminary Investigation of Flow Fluctuations During Surge and Blade Row Stall in Axial-Flow Compressors. NACA RM E52E28, 1952.

4. Huppert, Merle C., Johnson, Donald F., and Costilow, Eleanor L.: Preliminary Investigation of Compressor Blade Vibration Excited by Rotating Stall. NACA RM E52J15, 1952.

5. Huppert, Merle C., Costilow, Eleanor L., and Budinger, Ray E.: Investigation of a 10-Stage Subsonic Axial-Flow Research Compressor. III - Investigation of Rotating Stall, Blade Vibration, and Surge at Low and Intermediate Compressor Speeds. NACA RM E53C19, 1953.

6. Howell, A. R., and Carter, A. D. S.: Note on Stalling Flutter of Compressor Blades. Memo. No. 131, British N.G.T.E., Oct. 1951.

7. Carter, A. D. S., and Kilpatrick, D. A.: Preliminary Flutter Test on a Low Stagger Compressor Cascade. Memo. No. 141, British N.G.T.E., Jan. 1952.

8. Huppert, Merle C., and Benser, William A.: Some Stall and Surge Phenomenon in Axial-Flow Compressors. Jour. Aero. Sci., vol. 20, no. 12, Dec. 1953, pp. 835-845.

9. Howell, A. R.: The Present Basis of Axial Flow Compressor Design. Part I. Cascade Theory and Performance. R. & M. No. 2095, British A.R.C., June 1942.

10. Meyer, André J., Jr., and Calvert, Howard F.: Vibration Survey of Blades in 10-Stage Axial-Flow Compressor. II - Dynamic Investigation. NACA RM E8J22a, 1949. (Supersedes NACA RM E7D09.)

11. Laurence, James C., and Landes, L. Gene: Auxiliary Equipment and Technique for Adapting the Constant-Temperature Hot-Wire Anemometer to Specific Problems in Air-Flow Measurements. NACA TN 2843, 1952.

12. Manley, R. G.: Waveform Analysis. John Wiley & Sons, Inc., 1945.

13. Timoshenko, Stephen: Vibration Problems in Engineering. Second ed., D. Van Nostrand Co., Inc., 1937, p. 386.

TABLE I. - ENGINE CONFIGURATIONS

Engine configuration	Jet-nozzle size	Guide-vane assembly
1	Standard[a]	Guide vane A (fig. 1) (Standard[b])
2	4 Percent closed	
3	8 Percent closed	
4	12 Percent closed	
5	Standard	Guide vane B (fig. 1)
6	8 Percent closed	
7	8 Percent closed	Guide vane C (fig. 1) (1/2 standard solidity)

[a]Nozzle area resulting in rated turbine-outlet temperature at rated engine speed.

[b]Standard guide-vane assembly is that assembly furnished as standard part of engine.

TABLE II. - SUMMARY OF VIBRATORY STRESSES OBTAINED IN FIRST-STAGE ROTOR BLADES

[The stresses listed are those measured in three or more standard first-stage rotor blades during several vibration bursts. Maximum, average, and minimum values refer to the maximum stress measured over a period of time among the blades under observation.]

Configuration number	Vibratory stress in speed range of 60 to 63 percent of rated speed, psi			Vibratory stress in speed range of 70 to 72 percent of rated speed, psi		
	Maximum	Average	Minimum	Maximum	Average	Minimum
1	±13,500[a]	±11,700[a]	±8,800[a]	±4,000		
2	±10,800	±9,400	±8,800	±24,800	±17,000	±14,400
3	±19,400	±12,800	±9,400	±21,800	±16,900	±6,200
4	±9,200	±6,600	±4,400	±34,800	±27,000	±22,200
5	±28,000	±18,800	±13,400	±4,000		
6	±24,600	±18,000	±14,000	±16,600	±13,800	±10,500
7	±15,800	±13,600	±10,100	±26,800	±20,800	±13,700

[a]Obtained during an engine acceleration.

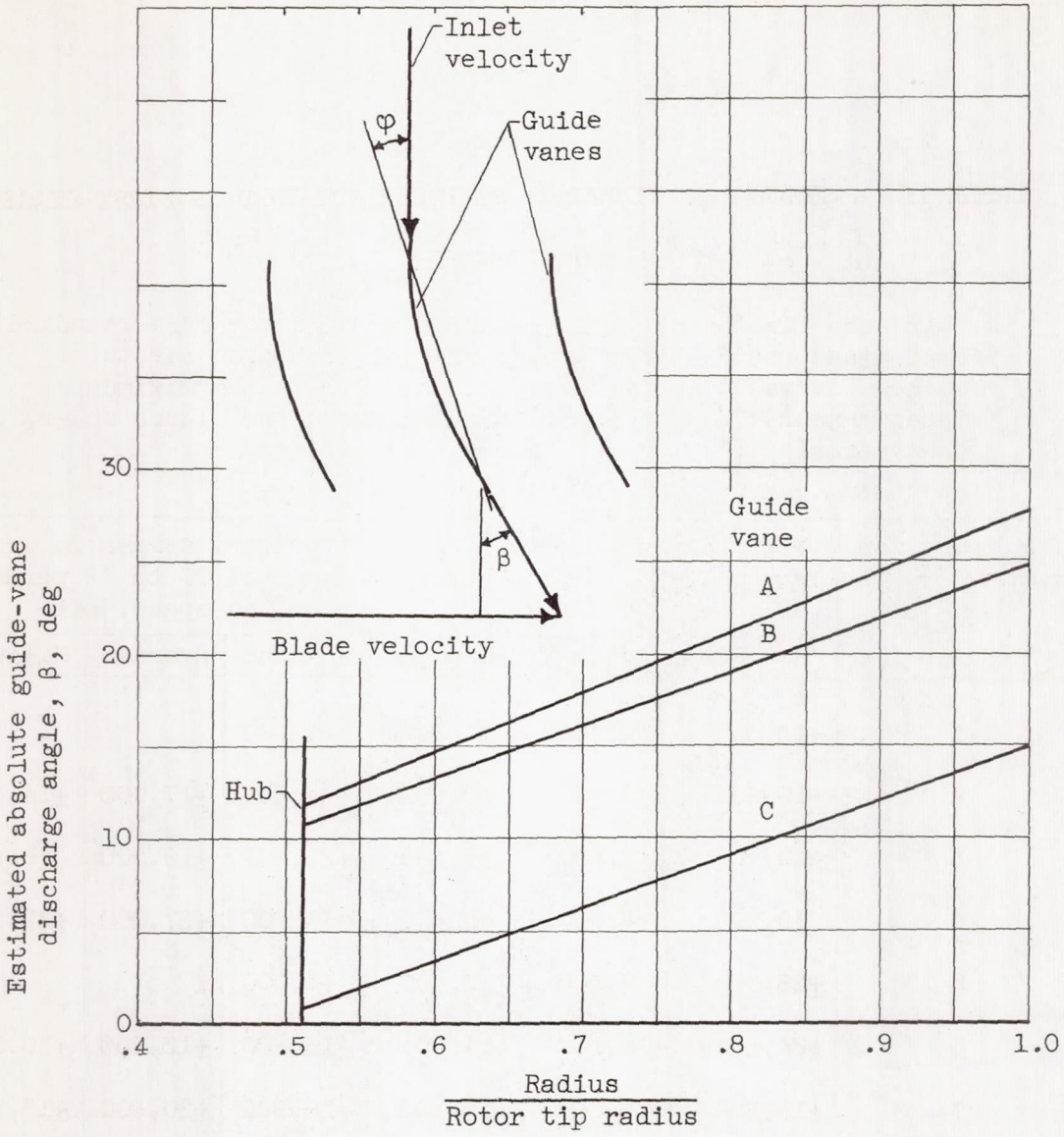


Figure 1. - Variation of guide-vane turning with radius ratio.

Guide vane	Solidity (all radii)	Setting angle, φ
A (std)	1.68	Design
B	.84	Design
C	.84	Design minus 10° (all radii)

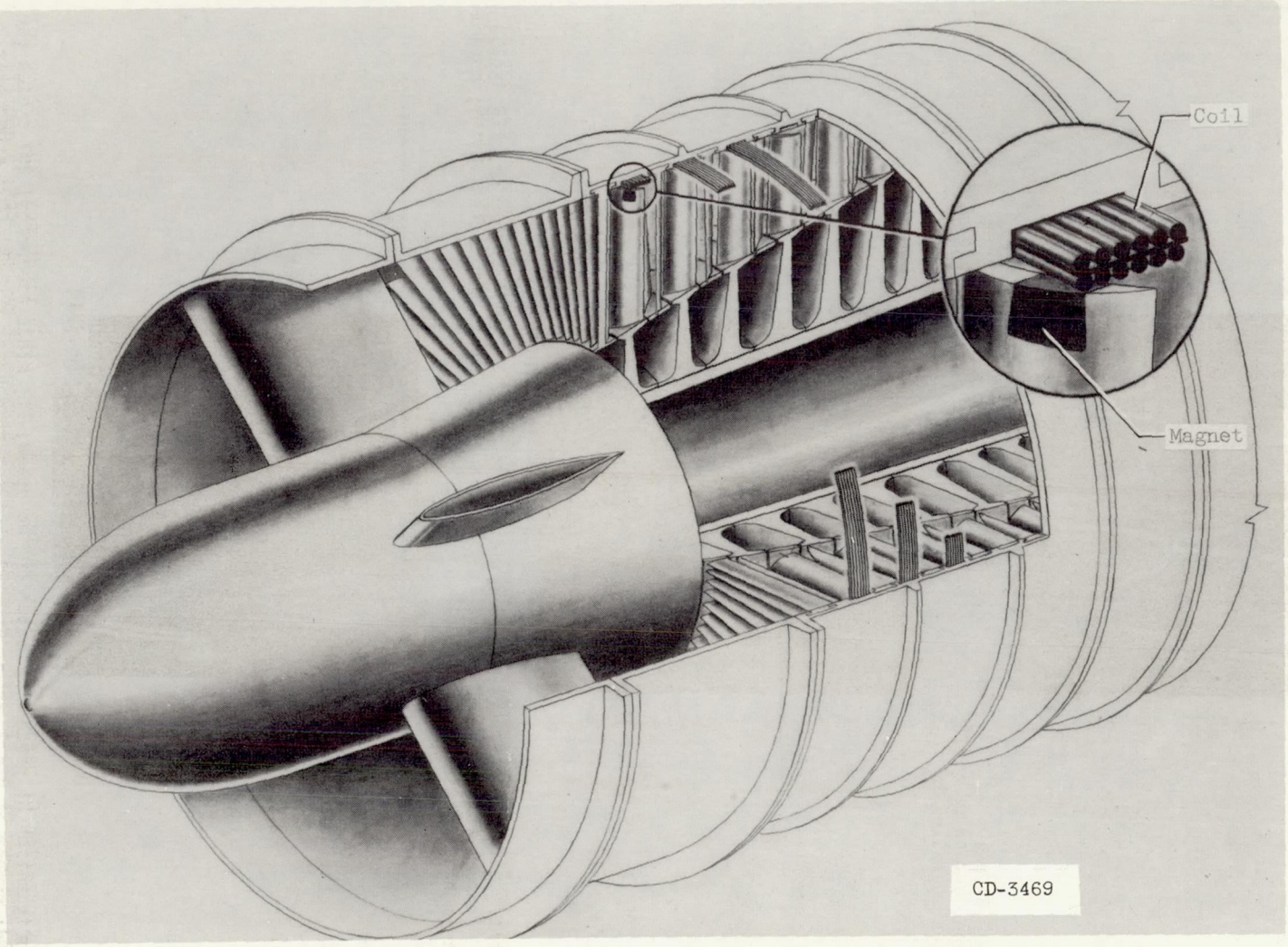
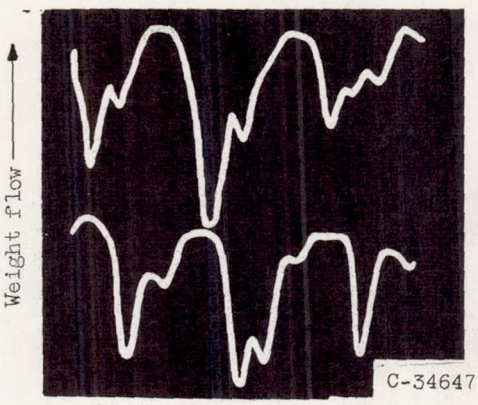
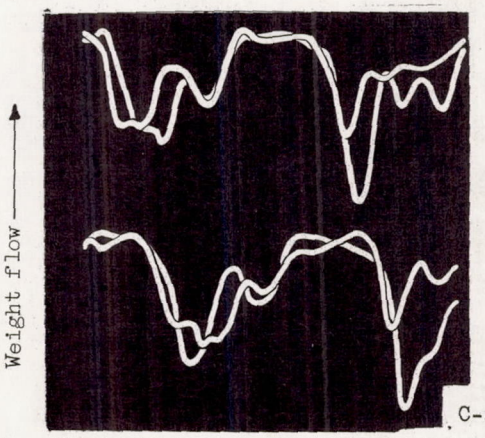


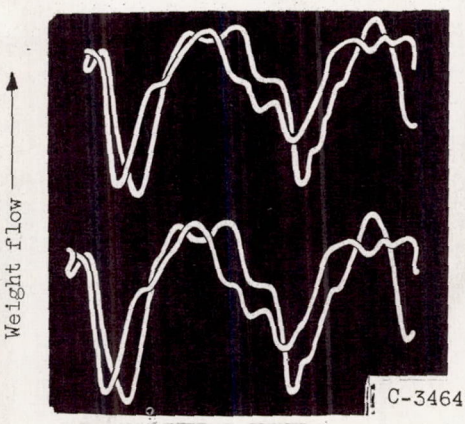
Figure 2. - Magnetic blade vibration indicator.



(a) Configuration 1; percent of rated engine speed, 65; stall frequency, 243 cycles per second; number of stall zones, 5; angle between anemometer probes, 24.6°; anemometer probes installed in third-stage stator.

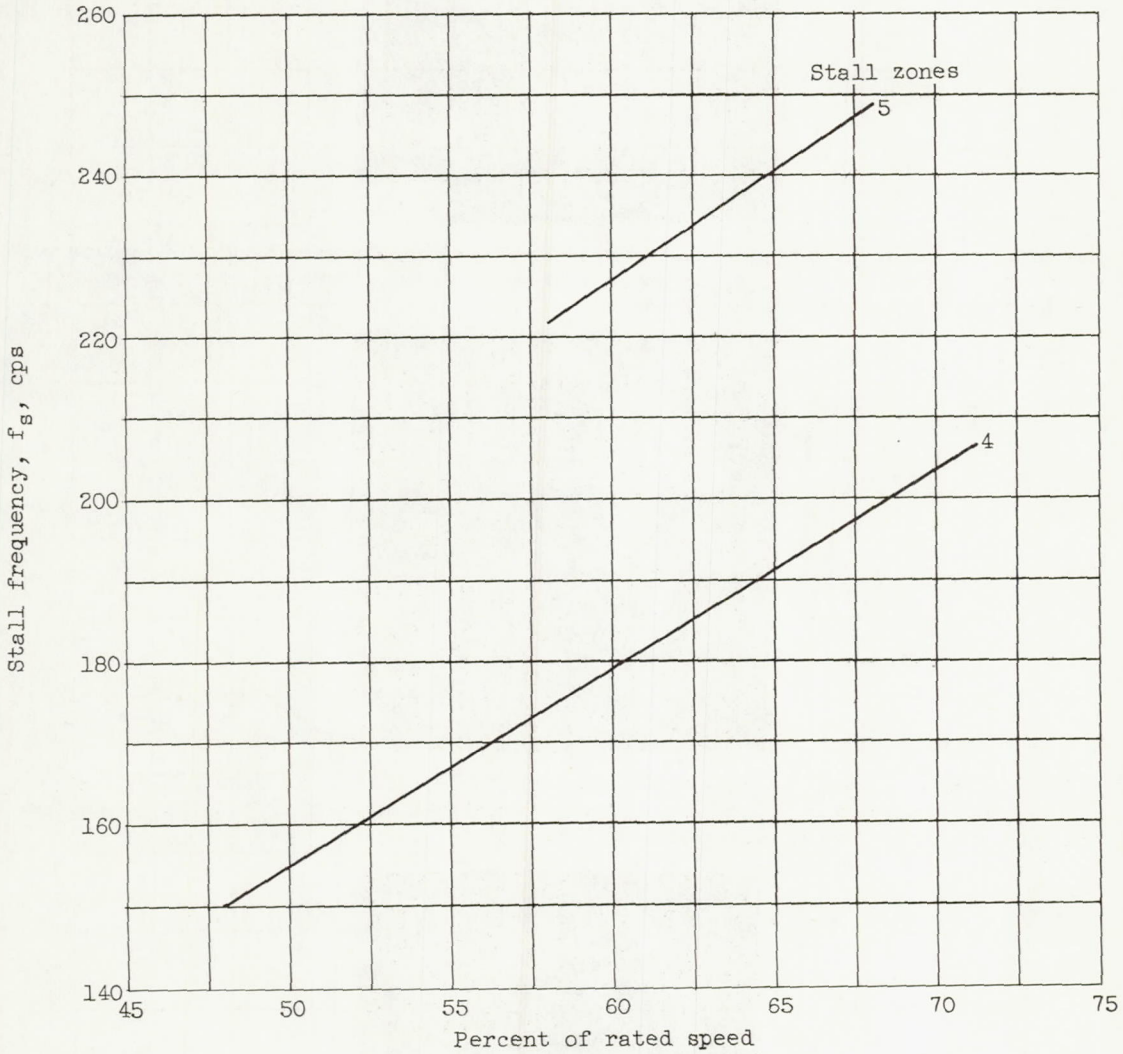


(b) Configuration 1; percent of rated engine speed, 67.5; stall frequency, 199 cycles per second; number of stall zones, 4; angle between anemometer probes, 24.6°; anemometer probes installed in third-stage rotor.



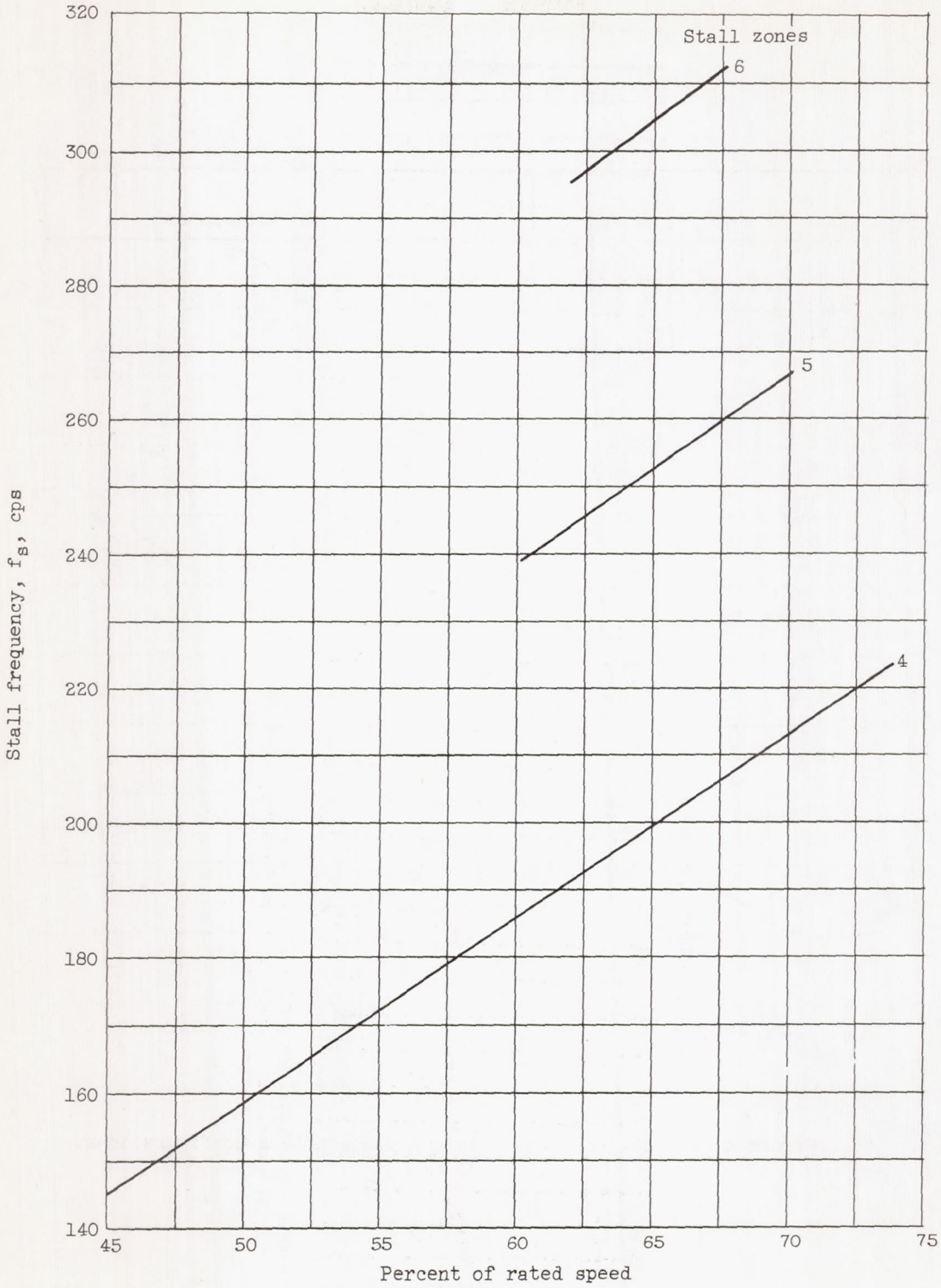
(c) Configuration 6; percent of rated engine speed, 65; stall frequency, 297 cycles per second; number of stall zones, 6; angle between anemometer probes, 60°; anemometer probes installed in first-stage stator.

Figure 3. - Oscillograms of hot-wire-anemometer signal. Radius ratio, 0.95; $\Delta\rho V/\rho V$; 1.0.



(a) Configuration 1.

Figure 4. - Stall patterns obtained with various configurations.



(b) Configuration 6.

Figure 4. - Concluded. Stall patterns obtained with various configurations.

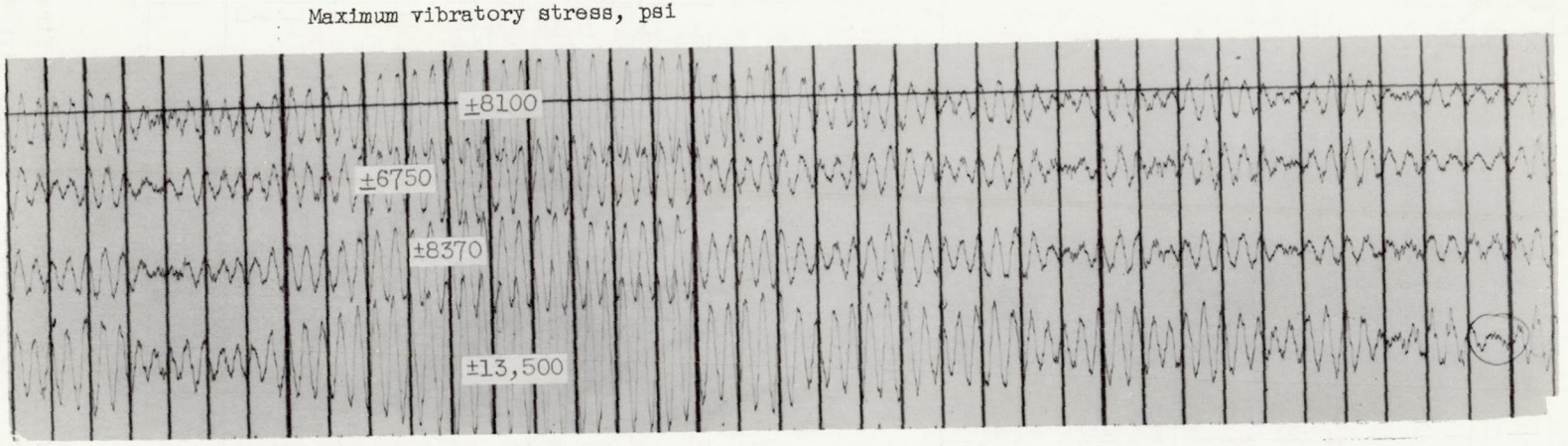


Figure 5. - Oscillogram of vibration burst during engine acceleration. Configuration 1; percent of radial engine speed, 62; blade vibration frequency, 231 cycles per second.

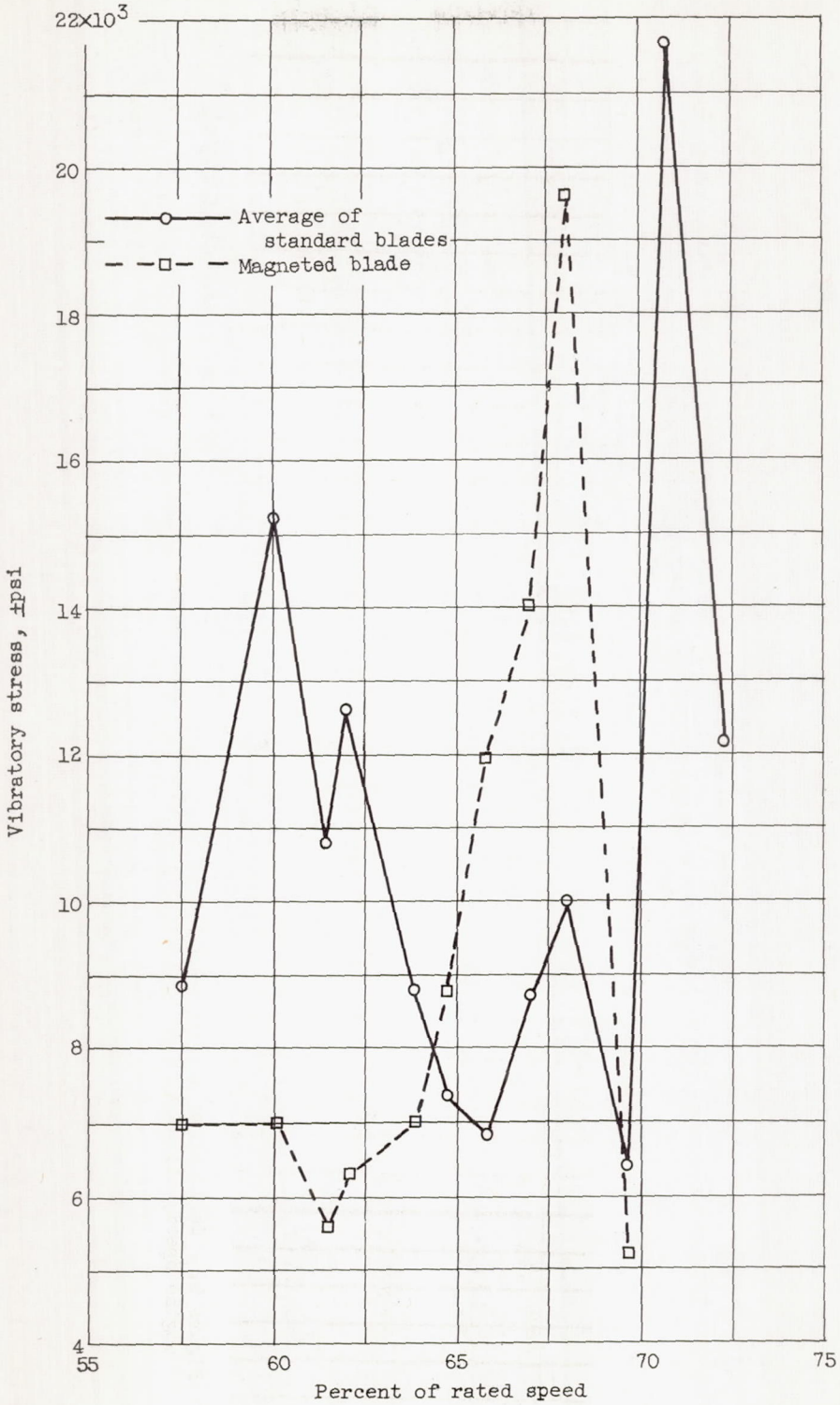


Figure 6. - Vibratory stress measured in first-stage rotor blades with configuration 3.

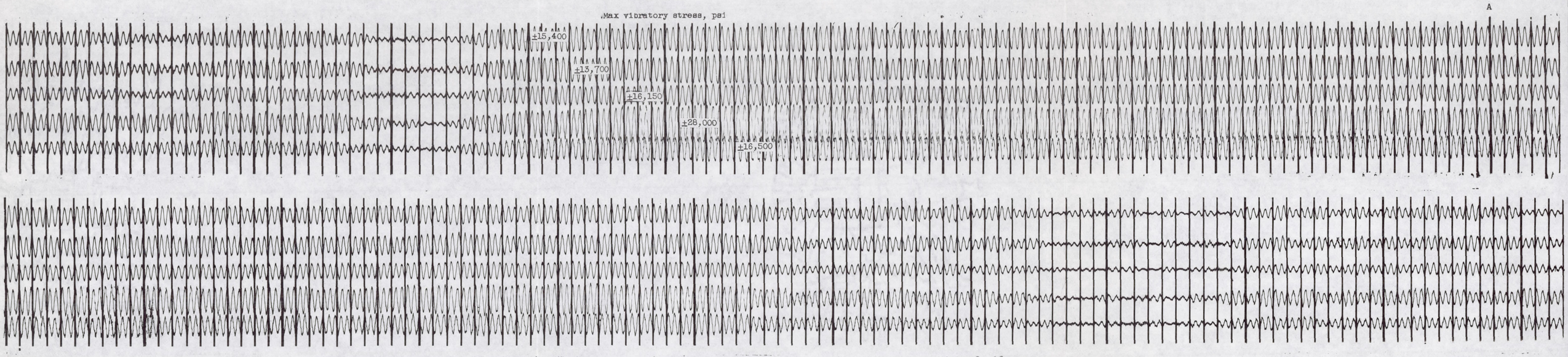


Figure 7. - Oscillogram of vibration burst caused by six-zone stall pattern. Configuration 5, percent of rated engine speed, 62; blade vibration frequency, 219 cycles per second.

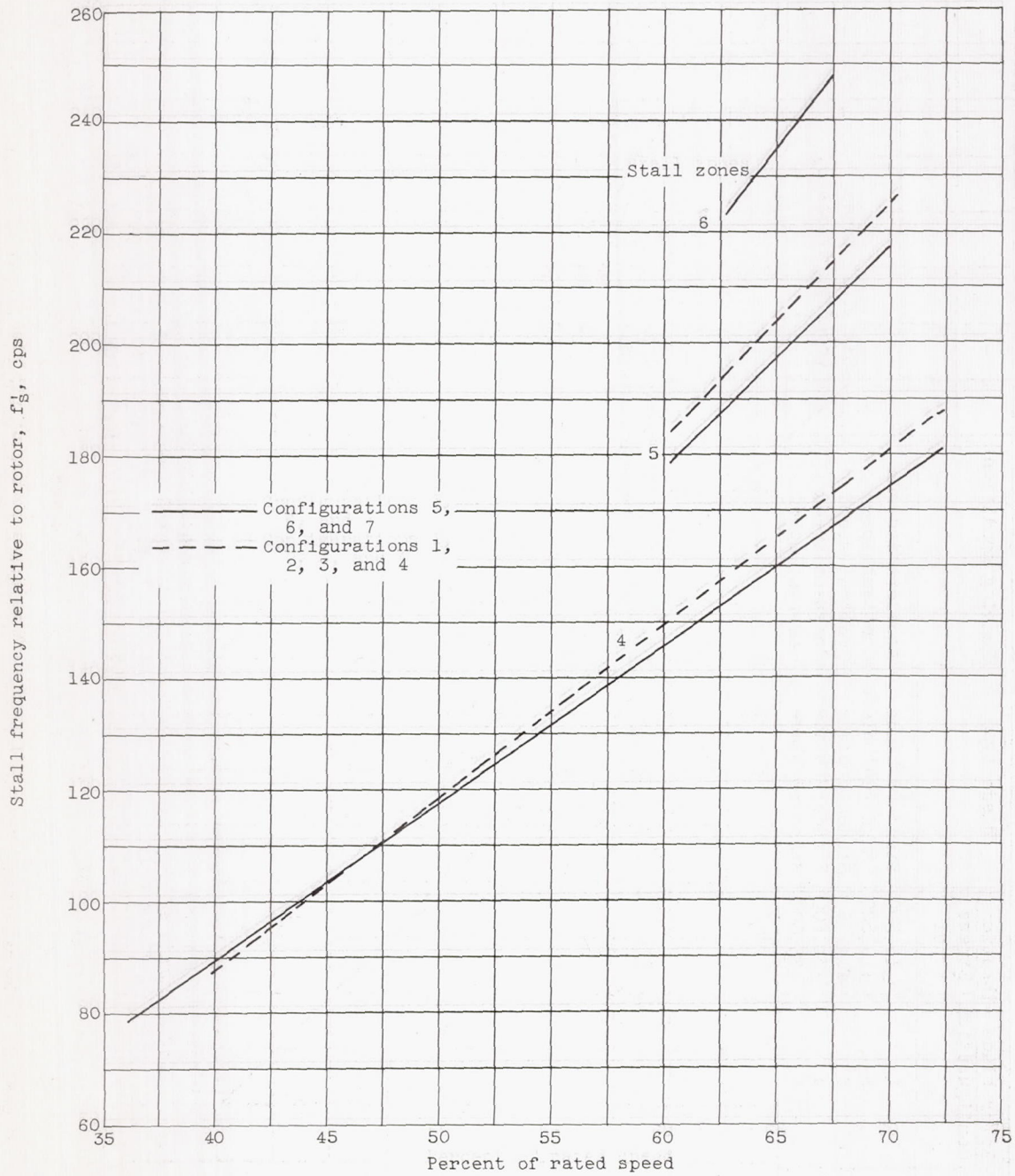


Figure 8. - Variation of stall frequency relative to rotor with percent of rated engine speed.

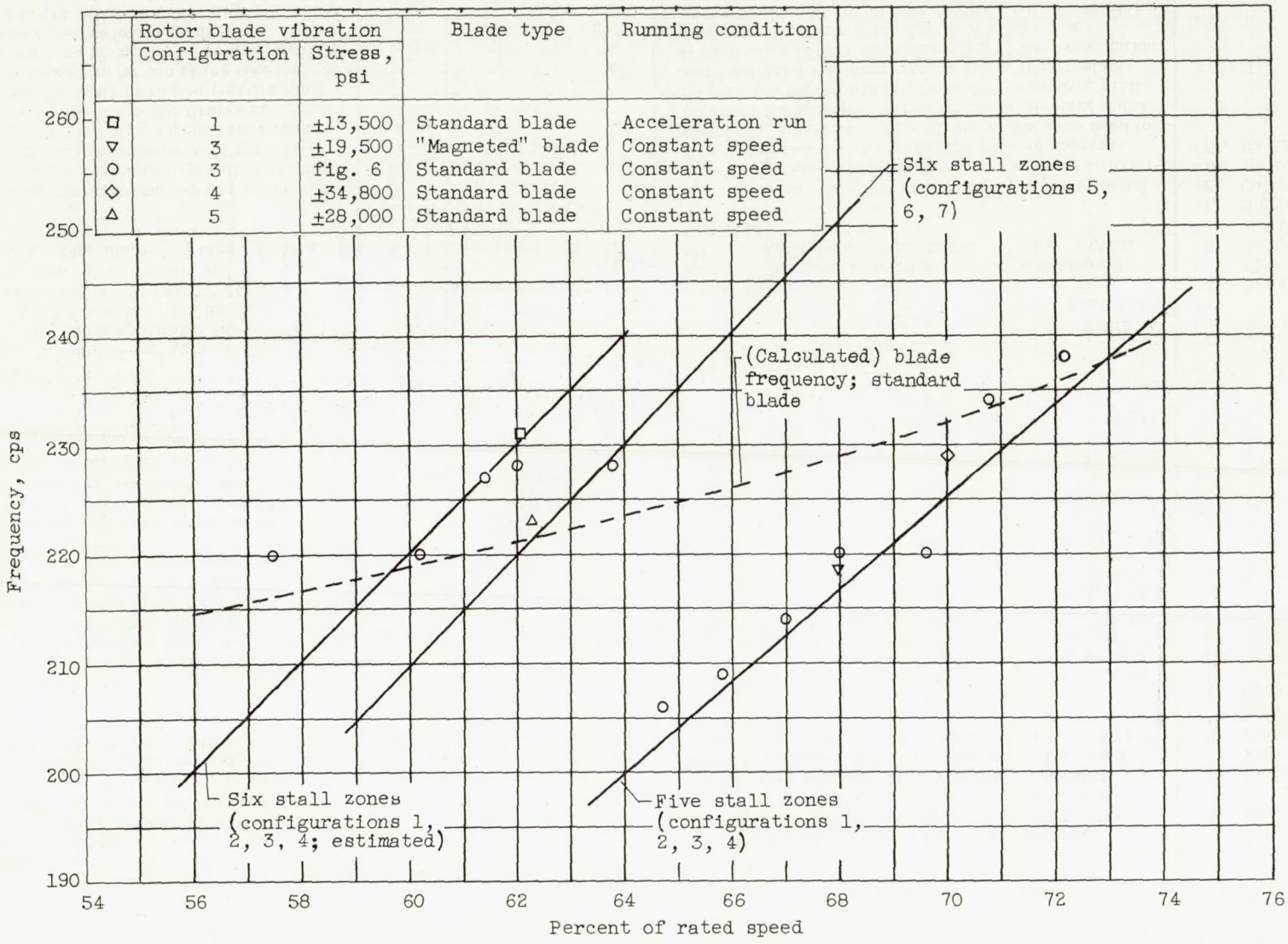


Figure 9. - Correlation of relative stall frequency with rotor-blade vibration frequency.